

## Research paper

# Mathematical model of brain tumour growth with drug resistance



José Trobia<sup>a</sup>, Kun Tian<sup>b</sup>, Antonio M Batista<sup>a,c,\*</sup>, Celso Grebogi<sup>b,d</sup>,  
 Hai-Peng Ren<sup>b,e</sup>, Moises S Santos<sup>f</sup>, Paulo R Protachevicz<sup>g</sup>, Fernando S Borges<sup>h</sup>,  
 José D Szezech Jr.<sup>a,c</sup>, Ricardo L Viana<sup>i</sup>, Iberê L Caldas<sup>g</sup>, Kelly C Iarosz<sup>f,j</sup>

<sup>a</sup> Department of Mathematics and Statistics, State University of Ponta Grossa, Ponta Grossa, 84030-900, PR, Brazil

<sup>b</sup> Shaanxi Key Lab of Complex System Control and Intelligent Information Processing, Xi'an University of Technology, Xi'an 710048, PR, China

<sup>c</sup> Graduate in Science Program - Physics, State University of Ponta Grossa, Ponta Grossa, 84030-900, PR, Brazil

<sup>d</sup> Institute for Complex Systems and Mathematical Biology, University of Aberdeen, Aberdeen, AB24 3UE, Scotland, United Kingdom

<sup>e</sup> Xi'an Technological University, Xi'an, 710021, PR, China

<sup>f</sup> Faculdade de Telêmaco Borba, FATEB, Telêmaco Borba, 84266-010, PR, Brazil

<sup>g</sup> Institute of Physics, University of São Paulo, São Paulo, 05508-900, SP, Brazil

<sup>h</sup> Center for Mathematics, Computation, and Cognition, Federal University of ABC, São Bernardo do Campo, 09606-045, SP, Brazil

<sup>i</sup> Department of Physics, Federal University of Paraná, Curitiba, 80060-000, PR, Brazil

<sup>j</sup> Graduate Program in Chemical Engineering Federal Technological University of Paraná, Ponta Grossa, 84017-220, PR, Brazil

## ARTICLE INFO

## Article history:

Received 4 May 2021

Revised 9 August 2021

Accepted 22 August 2021

Available online 31 August 2021

## Keywords:

Brain

Tumour

Chemotherapy

Drug resistance

Glia-neuron interaction

## ABSTRACT

Brain tumours are masses of abnormal cells that can grow in an uncontrolled way in the brain. There are different types of malignant brain tumours. Gliomas are malignant brain tumours that grow from glial cells and are identified as astrocytoma, oligodendroglioma, and ependymoma. We study a mathematical model that describes glia-neuron interaction, glioma, and chemotherapeutic agent. In this work, we consider drug sensitive and resistant glioma cells. We show how continuous and pulsed chemotherapy can kill glioma cells with a minimal loss of neurons.

© 2021 Elsevier B.V. All rights reserved.

## 1. Introduction

Tumour cells are abnormal cells that are classified into benign and malignant. The benign tumours do not invade the normal tissue, while the malignant tumour invade and can spread around the body [1]. The malignant tumours are cancerous tumours and they have a growth rate much faster than normal cells [2,3]. Cancer is one of the main causes of death worldwide and many treatments have been developed, such as chemotherapy, radiation therapy, and surgery [4].

Mathematical modelling of tumour growth has been used to understand different aspects of cancer [5–7]. Pinho et al. [8] analysed a mathematical model of cancer treatment by chemotherapy agent taking metastasis into account. Borges et al. [9] used a model to study tumour growth under treatment by continuous and pulsed chemotherapy. Nani and Freedman

\* Corresponding author at: Department of Mathematics and Statistics, State University of Ponta Grossa, 84030-900, Ponta Grossa, PR, Brazil.  
 E-mail addresses: [abatista@uepg.br](mailto:abatista@uepg.br) (A.M. Batista), [kiarosz@gmail.com](mailto:kiarosz@gmail.com) (K.C. Iarosz).

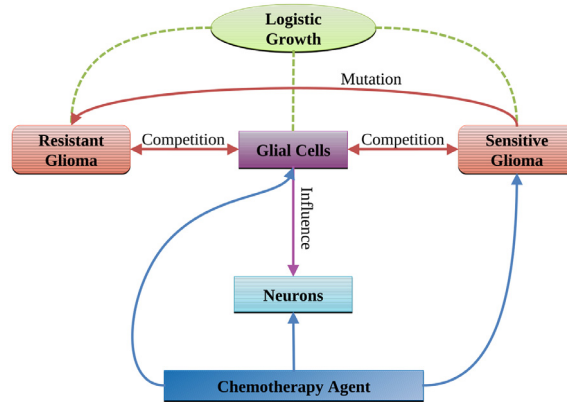


Fig. 1. Schematic representation of the model.

[10] studied cancer immunotherapy through models that incorporate tumor-immune interaction [11]. Behera and O'Rourke [12] studied the effect of noise in a tumour growth model. It was showed that noise can affect the stability of the dynamic system [13–19]. One of the most common type of malignant brain tumour is the glioma that starts in the glial cells [20]. The glial cells provide neuronal support and protection [21].

Drug resistance in cancer is a major problem in chemotherapy treatment [22], due to the ability of cancerous cells to develop resistance to chemotherapeutic agents [23]. Nass and Efferth [24] studied drug targets and resistance mechanisms in myeloma. Recently, He et al. [25] reported mechanisms related to drug-resistant ovarian-cancer cells. In the literature, it is possible to find different brain tumour models. Partial [26] and ordinary [27] differential equations have been used to simulate the dynamic behaviour related to the glioma growth. A mathematical modelling of therapy, inducing cancer drug resistance, was analysed by Sun et al. [28].

Chemoresistance profiles for brain tumours were studied by Haroun et al. [29] by means of tumour specimens collected from various patients. The tumours were analysed in vitro against different chemotherapeutic agents. They reported extreme drug resistance in primary tumours, for instance, glioblastomas and astrocytomas exhibited resistance to paclitaxel and carboplatin, respectively. We propose a model with tumour drug resistance by adding a new differential equation in the model proposed by Iarosz et al. [30] for gliomas with glia-neuron interactions and chemotherapy treatment. Our model is able to reproduce the same behaviour that was experimentally observed by Rabé et al. [31] in their studies about the temozolomide resistance in glioblastoma.

In this way, our model has glia-neuron interactions, resistant and sensitive gliomas, as well as chemotherapy treatment. The tumour treatment occurs through continuous or pulsed chemotherapy. We computed the values of the infusion of chemotherapy agents in which the glioma is suppressed and a minimum number of neurons is lost, without neurogenesis. In the continuous chemotherapy, the neuronal lifespan depends on the infusion of chemotherapy agent rate and the mutation rate from drug-sensitive to drug-resistant cells. With regard to the pulsed chemotherapy, we show that the chemotherapy cycle and the time interval of the drug application play a crucial role in the glioma treatment.

This paper is organised as follows: in Section 2, we introduce the mathematical model; Section 3 presents our results for continuous and pulsed chemotherapy; we draw our conclusions in Section 4.

## 2. Brain tumour model with drug resistance

We include drug resistance in the model proposed in [30]. Fig. 1 displays a schematic representation of the interactions considered in the modified model. The sensitive and resistant glioma cells have logistic growth, allowing for the action on the glial cells and for the influence on the neurons. The glial cells interact with the neurons and the glioma cells, having a logistic growth. The chemotherapy agent is a predator that affects the glioma cells, glial cells, and neurons. Due to the chemotherapy, the sensitive glioma cells convert to resistant glioma cells through mutations.

The mathematical model considered in this work is described by

$$\frac{dG(t)}{dt} = P_G G(t) \left( 1 - \frac{G(t)}{C_1} \right) - \Psi_G G(t) [S(t) + R(t)] - \frac{I_1 G(t) Q(t)}{A_1 + G(t)}, \quad (1)$$

$$\frac{dS(t)}{dt} = P_S S(t) \left( 1 - \frac{S(t) + R(t)}{C_2} \right) - \Psi_S G(t) S(t) - uF[Q(t)]S(t) - \frac{I_2 S(t) Q(t)}{A_2 + S(t)}, \quad (2)$$

$$\frac{dR(t)}{dt} = P_R R(t) \left( 1 - \frac{S(t) + R(t)}{C_2} \right) - \Psi_R G(t) R(t) + uF[Q(t)]S(t), \quad (3)$$

**Table 1**  
Parameters values taken from the referenced literature.

Parameter	Values	Description
$P_G$	0.0068 day <sup>-1</sup>	
$P_S$	0.012 day <sup>-1</sup>	Proliferation rate [32,33]
$P_R$	0.002 and 0.006 day <sup>-1</sup>	
$\psi$	0 – 0.02	Loss influences [32]
$I_1, I_3$	$2.4 \times 10^{-5}$ m <sup>2</sup> (mg.day) <sup>-1</sup>	Interaction
$I_2$	$2.4 \times 10^{-2}$ m <sup>2</sup> (mg.day) <sup>-1</sup>	coefficients [32,34]
$\Phi$	0 – 200 mg(m <sup>2</sup> .day) <sup>-1</sup>	Chemotherapy [35,36]
$\zeta$	0.2 day <sup>-1</sup>	Absorption rate [9]
$u$	0 – 1	Mutation rate
$A_1, A_2, A_3$	510 kg.m <sup>-3</sup>	Holling type 2
$\Psi_G$	$3.6 \times 10^{-5}$ day <sup>-1</sup>	Competition
$\Psi_S, \Psi_R$	$3.6 \times 10^{-6}$ day <sup>-1</sup>	coefficients [32]
$C_1, C_2, C_3$	510 kg.m <sup>-3</sup>	Carrying capacity [37]

$$\frac{dN(t)}{dt} = \psi \dot{G}(t)F\left(-\frac{\dot{G}(t)}{C_1}\right)N(t) - \frac{I_3 N(t)Q(t)}{A_3 + N(t)}, \tag{4}$$

$$\frac{dQ(t)}{dt} = \Phi - \zeta Q(t), \tag{5}$$

where  $G$  is the glial cells concentration (kg.m<sup>-3</sup>),  $S$  is the drug sensitive glioma cells concentration (kg.m<sup>-3</sup>),  $R$  is the drug resistant glioma cells concentration (kg.m<sup>-3</sup>),  $N$  is the neurons concentration (kg.m<sup>-3</sup>),  $Q$  is the chemotherapeutic agent concentration (mg.m<sup>-2</sup>), and  $F(x)$  is a function defined as

$$F(x) = \begin{cases} 0, & x \leq 0, \\ 1, & x > 0. \end{cases} \tag{6}$$

Table 1 describes the values of the parameters taken from the cited references. In Eqs. (2) and (3), the third term is related to the change from sensitive to resistant glioma cells. In Eq. (4), the first term is associated with the decay of the neuronal population due to the glial cells death.

The normalised model is given by

$$\frac{dg(t)}{dt} = P_G g(t)[1 - g(t)] - \beta_1 g(t)[s(t) + r(t)] - \frac{i_1 g(t)q(t)}{a_1 + g(t)}, \tag{7}$$

$$\frac{ds(t)}{dt} = P_S s(t)[1 - (s(t) + r(t))] - \beta_2 g(t)s(t) - uF[q(t)]s(t) - \frac{i_2 s(t)q(t)}{a_2 + s(t)}, \tag{8}$$

$$\frac{dr(t)}{dt} = P_R r(t)[1 - (s(t) + r(t))] - \beta_3 g(t)r(t) + uF[q(t)]s(t), \tag{9}$$

$$\frac{dn(t)}{dt} = \alpha \dot{g}(t)F[-\dot{g}(t)]n(t) - \frac{i_3 n(t)q(t)}{a_3 + n(t)}, \tag{10}$$

$$\frac{dq(t)}{dt} = \Phi - \zeta q(t), \tag{11}$$

where  $g(t) = \frac{G(t)}{C_1}$ ,  $s(t) = \frac{S(t)}{C_2}$ ,  $r(t) = \frac{R(t)}{C_2}$ ,  $n(t) = \frac{N(t)}{C_3}$ ,  $\beta_1 = \Psi_G C_2$ ,  $\beta_2 = \Psi_S C_1$ ,  $\beta_3 = \Psi_R C_1$ ,  $\alpha = \psi C_1$ ,  $a_i = \frac{A_i}{C_i}$ ,  $i_i = \frac{I_i}{C_i}$  ( $i = 1, 2, 3$ ), and  $q(t) = Q(t)$ . The values of the parameters are given in Table 2.

**Table 2**  
Values of the parameters for the normalisation.

Parameter	Values
$\beta_1$	$1.8 \times 10^{-2}$ day <sup>-1</sup>
$\beta_2, \beta_3$	$1.8 \times 10^{-3}$ day <sup>-1</sup>
$\alpha$	0 – 10
$a_1, a_2, a_3$	1
$i_1, i_3$	$4.7 \times 10^{-8}$ m <sup>2</sup> (mg.day) <sup>-1</sup>
$i_2$	$4.7 \times 10^{-5}$ m <sup>2</sup> (mg.day) <sup>-1</sup>

The equilibria points, which are physiologically feasible,  $E(g, s, r, n, q)$  of the model are obtained by setting  $\dot{g}(t) = 0, \dot{s}(t) = 0, \dot{r}(t) = 0, \dot{n}(t) = 0,$  and  $\dot{q}(t) = 0$ . We analyse next the local stability of an equilibrium given by  $E_0(0, 0, 0, 0, \Phi\zeta^{-1})$ . The eigenvalues of the Jacobian matrix are

$$\lambda_1^{(0)} = P_G - \frac{i_1\Phi}{\zeta a_1}, \tag{12}$$

$$\lambda_2^{(0)} = P_S - \frac{i_2\Phi}{\zeta a_2} - u, \tag{13}$$

$$\lambda_3^{(0)} = P_R, \tag{14}$$

$$\lambda_4^{(0)} = -\frac{i_3\Phi}{\zeta a_3}, \tag{15}$$

$$\lambda_5^{(0)} = -\zeta. \tag{16}$$

We identify the stability of the equilibrium through the sign of the real part of each eigenvalue. If the real part of each eigenvalue is strictly negative, then the equilibrium is locally asymptotically stable, and if positive, then the equilibrium is unstable. In order to ensure the stability of  $E_0(0, 0, 0, 0, \Phi\zeta^{-1})$ , it is necessary that

$$\Phi > \frac{P_G a_1 \zeta}{i_1}, \tag{17}$$

$$\Phi > \frac{(P_S - u) a_2 \zeta}{i_2}, \tag{18}$$

which are obtained by requiring that  $\lambda_1^{(0)} < 0$  and  $\lambda_2^{(0)} < 0$ . The values of the normalised parameters are positive (Table 2), then the eigenvalues  $\lambda_4^{(0)}$  and  $\lambda_5^{(0)}$  are negative. However, the eigenvalue  $\lambda_3^{(0)}$  is positive. Therefore, the equilibrium  $E_0(0, 0, 0, 0, \Phi\zeta^{-1})$  is unstable due to the fact that the drug resistant glioma cells are not affected by the chemotherapeutic agent. It is possible to find a stable equilibrium  $E_1(0, 0, r^*, 0, \Phi\zeta^{-1})$  for  $r^* = 1$ . The eigenvalues of the Jacobian matrix are

$$\lambda_1^{(1)} = P_G - \beta_1 - \frac{i_1\Phi}{\zeta a_1}, \tag{19}$$

$$\lambda_2^{(1)} = -\frac{i_2\Phi}{\zeta a_2} - u, \tag{20}$$

$$\lambda_3^{(1)} = -P_R, \tag{21}$$

$$\lambda_4^{(1)} = -\frac{i_3\Phi}{\zeta a_3}, \tag{22}$$

$$\lambda_5^{(1)} = -\zeta. \tag{23}$$

In order to ensure the stability of  $E_1(0, 0, r^*, 0, \Phi\zeta^{-1})$ , it is necessary that

$$\Phi > \frac{(P_G - \beta_1) a_1 \zeta}{i_1}, \tag{24}$$

by requiring that  $\lambda_1^{(0)} < 0$ . The eigenvalues  $\lambda_2^{(0)}, \lambda_3^{(0)}, \lambda_4^{(0)},$  and  $\lambda_5^{(0)}$  are negative because the values of the normalised parameters are positive. We consider  $a_1 = 1, P_G = 0.0068, \beta_1 = 0.018, i_1 = 4.7 \times 10^{-8},$  and  $\zeta = 0.2$  (Table 2). With these values, we obtain that  $E_1$  is linearly asymptotically stable for  $\Phi > -47,659$ . Therefore, when the chemotherapeutic agent kills all glial cells ( $g$ ) and drug sensitive glioma cells ( $s$ ), the normalised drug resistant glioma cells concentration is  $r = 1$ . Although there is no case where the concentrations of glial cells and neurons are both equal to zero, it is interesting to analyse the stability of the equilibria  $E_0$  and  $E_1$  to learn the values of the chemotherapy concentrations that could happen. This analysis gives us the maximum chemotherapy values that can be used without killing all the glial cells and neurons.

We also consider the equilibrium  $E_2(\bar{g}, 0, 0, \bar{n}, \bar{q})$  that represents the complete elimination of drug sensitive glioma cells and drug resistant glioma cells, though the glial and neuron cells are preserved. This equilibrium is obtained by the solution of

$$P_G(1 - \bar{g}) - \frac{i_1\bar{q}}{a_1 + \bar{g}} = 0, \tag{25}$$

$$-\frac{i_3\bar{n}\bar{q}}{a_3 + \bar{n}} = 0, \tag{26}$$

$$\Phi - \zeta\bar{q} = 0, \tag{27}$$

for  $\bar{n} = 0$  and  $\bar{q} = \Phi\zeta^{-1}$ . Thus, the equilibrium  $E_2(\bar{g}, 0, 0, \bar{n}, \bar{q})$  is given by  $E_2(\bar{g}, 0, 0, 0, \Phi\zeta^{-1})$ , meaning that all neurons are also eliminated. Eq. (25) can be rewritten as

$$\bar{g}^2 + \bar{g}(a_1 - 1) - a_1 + \frac{i_1\Phi}{\zeta P_G} = 0. \tag{28}$$

Using the parameters of Table 1 and 2,  $\bar{g}$  has a real, positive and non-null solution when  $\Phi < 28,936$ . The eigenvalues of the Jacobian matrix for  $E_2$  are

$$\lambda_1^{(2)} = P_G(1 - 2\bar{g}) - \frac{i_1 a_1 \Phi}{\zeta (a_1 + \bar{g})^2}, \tag{29}$$

$$\lambda_2^{(2)} = P_S - \beta_2 \bar{g} - u - \frac{i_2 \Phi}{\zeta a_2}, \tag{30}$$

$$\lambda_3^{(2)} = P_R - \beta_3 \bar{g}. \tag{31}$$

$$\lambda_4^{(2)} = -\frac{i_3 \Phi}{\zeta a_3}, \tag{32}$$

$$\lambda_5^{(2)} = -\zeta. \tag{33}$$

For  $a_1 = 1$ ,  $\lambda_1^{(2)}$  is negative in Eq. (29) when

$$(1 + \bar{g})^2(1 - 2\bar{g}) < \frac{i_1 \Phi}{\zeta P_G}. \tag{34}$$

From Eq. (28), it is obtained that  $\frac{i_1 \Phi}{\zeta P_G} = 1 - \bar{g}^2$ . Consequently

$$(1 - \bar{g}^2) - 2\bar{g}^2 - 2\bar{g}^3 < (1 - \bar{g}^2). \tag{35}$$

Therefore  $\lambda_1^{(2)} < 0$  if  $\bar{g} > 0$ .  $\lambda_2^{(2)}$  is negative for combinations of  $u$  and  $\Phi$ , for example: i)  $u = 0$  and  $\Phi > 43.41$ , ii)  $u = 0.001$  and  $\Phi > 39.15$ , and iii)  $u = 0.01$  and  $\Phi > 0.85$ . The values of  $\lambda_4^{(2)}$  and  $\lambda_5^{(2)}$  are negative. However,  $\lambda_3^{(0)}$  is positive if  $P_R > \beta_3$ . Using the parameters from Tables 1 and 2, we obtain  $\beta_3 = 0.0018$  and  $P_R \geq 0.002$ . For realistic parameters, the equilibrium  $E_2$  is unstable due to the fact that the proliferation rate of the drug resistant glioma cells is larger than the normalized competition between glioma and drug resistant glioma cells.

The equilibrium  $E_2$ , which is related to the elimination of all glioma cells, is unstable. In this case, all neurons are also eliminated, showing that it is unattainable to find a cure for glioma in the drug resistant case. For this reason, we focus on the neuronal lifespan during the chemotherapeutic treatment.

### 3. Chemotherapy treatment

#### 3.1. Continuous chemotherapy

Continuous infusion [38] followed by radiotherapy was used as a treatment for malignant tumour. Many researchers reported that this combination can improve the tumours' regression [39,40]. We consider continuous chemotherapy as a way to eliminate glioma cells having drug resistance. We show that our model presents a similar behaviour, recently reported by Rabé et al. [31]. They performed studies about the temozolomide resistance in glioblastoma by considering a combination of mathematical models, RNA sequencing, single cell analyses, functional and drug essays in a human glioma cell line. They identified a transient resistance state in which the cancerous cells have a reduced proliferation rate. We verify that our model is able to reproduce a transient resistance state, as shown in Fig. 2. For  $u = 10^{-2}$  (black line), the glioma cells ( $r(t) + s(t)$ ) initially decrease, though in accordance with [31], they do increase due to the drug resistance. For  $u = 0$  (blue line) and  $u = 10^{-3}$  (red line), the glial cells kill the drug sensitive and resistant glioma cells.

We show that our model presents a similar behaviour, recently reported by Rabé et al. [31]. They analysed mathematical models and performed drug assays in a human glioma cell line to study the resistance to temozolomide. Fig. 2 displays that glioma cells ( $r(t) + s(t)$ ) initially decrease, though, in accordance with [31] they should increase due to the drug resistance, see the black line.

Fig. 3 shows the time evolution of normalised (a) glial cells concentration  $g(t)$ , (b) neurons concentration  $n(t)$ , (c) drug sensitive glioma cells concentration  $s(t)$ , and (d) drug resistant glioma cells concentration  $r(t)$ . We consider  $\Phi = 200$ ,  $P_R = 0.002$ ,  $u = 0$  (blue line),  $u = 10^{-3}$  (red line), and  $u = 10^{-2}$  (black line). The chemotherapeutic agent kills the glial cells, neurons, and sensitive glioma cells. For  $u = 0$ , there is not resistant glioma and, as a consequence, the malignant tumour is suppressed. However, the neuron concentration  $n$  decreases slightly from 1 to 0.981 for  $t = 360$  days (12 months) (green vertical dashed line) and to 0.977 for  $t = 540$  days (18 months) (orange vertical dashed line). The glial cells undergo a necrosis by the chemotherapy in spite of exhibiting logistic growth. For  $u = 10^{-3}$ ,  $n$  decreases also slightly to 0.980 and 0.976 for

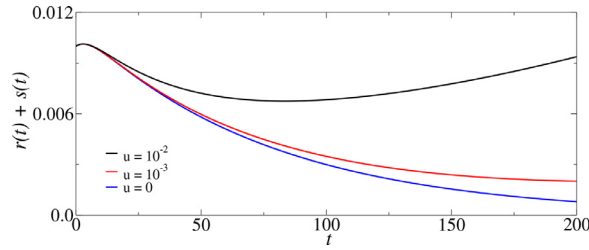


**Fig. 2.** Time evolution of  $r(t) + s(t)$  for  $\Phi = 50$ ,  $P_R = 0.002$ , and mutation rate  $u = 0$  (blue line),  $u = 10^{-3}$  (red line), and  $u = 10^{-2}$  (black line). We consider  $g(0) = 1$ ,  $n(0) = 1$ ,  $s(0) = 0.01$ , and  $r(0) = 0$ . (For interpretation of the references to color in this figure legend, the reader is referred to the web version of this article.)

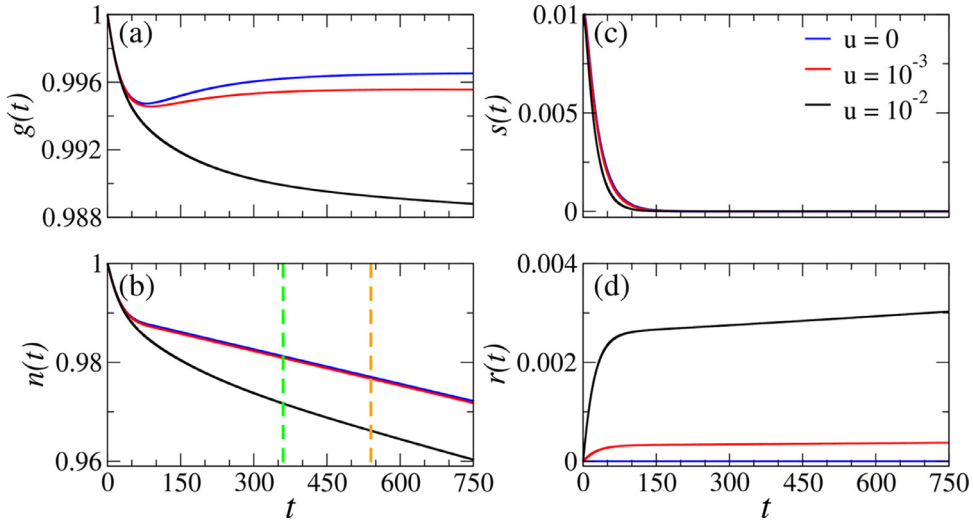


**Fig. 3.** Time evolution of (a) glial cells concentration  $g(t)$ , (b) neurons concentration  $n(t)$ , (c) drug sensitive glioma cells concentration  $s(t)$ , and (d) drug resistant glioma cells concentration  $r(t)$  for  $\Phi = 200$ ,  $P_R = 0.002$ , and mutation rate  $u = 0$  (blue line),  $u = 10^{-3}$  (red line), and  $u = 10^{-2}$  (black line). The green and orange vertical dashed lines correspond to 360 days (12 months) and 540 days (18 months), respectively. We consider  $g(0) = 1$ ,  $n(0) = 1$ ,  $s(0) = 0.01$ ,  $r(0) = 0$ , and  $q(0) = 0$ . (For interpretation of the references to color in this figure legend, the reader is referred to the web version of this article.)

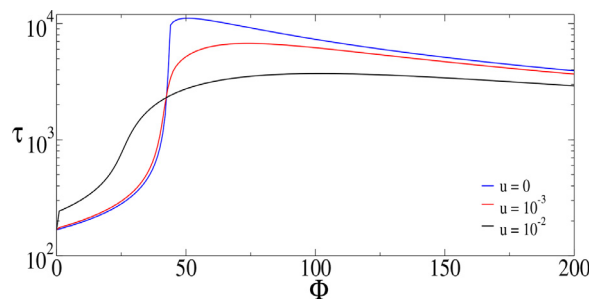


**Fig. 4.**  $\tau$  as a function of  $\Phi$  for  $P_R = 0.002$ ,  $u = 0$  (blue line),  $u = 10^{-3}$  (red line), and  $u = 10^{-2}$  (black line). (For interpretation of the references to color in this figure legend, the reader is referred to the web version of this article.)

360 and 540 days, respectively. Considering  $u = 10^{-2}$ , we observe  $n = 0.971$  for  $t = 360$  days, and  $n = 0.966$  for  $t = 540$  days. Importantly, the sensitive glioma cells are absent for  $t$  greater than approximately 150 days.

According to Peters et al. [41], there is an overall age-related loss of neurons, about 10%, from the cerebral cortex. With this in mind, we compute the time  $\tau$  in which the brains of patients with glioma have a loss of 10% in the neurons concentration ( $n = 0.9$ ). Fig. 4 shows the time  $\tau$  for a neuron to achieve the concentration  $n = 0.9$  as a function of  $\Phi$ . For  $u = 0$  (blue line) and  $\Phi = 200$ ,  $\tau$  is equal to 3926 days, while  $\tau$  is much less for  $u = 10^{-3}$  (red line) and  $u = 10^{-2}$  (black line). We obtain  $\tau$  equal to 3672 and 2910 days for  $u$  equal to  $10^{-3}$  and  $10^{-2}$ , respectively. Then, it is possible to conclude that  $u$  has an important effect on  $\tau$ .

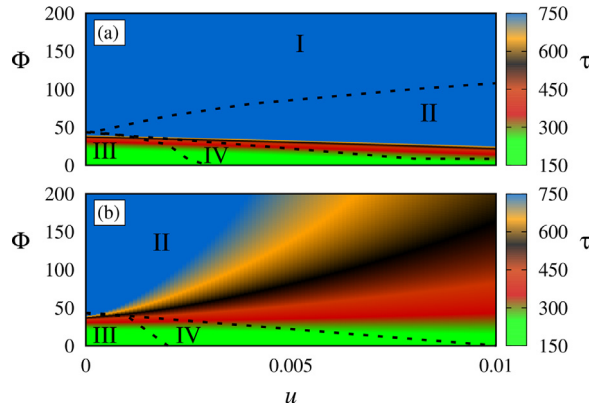


Fig. 5. Parameter space  $\Phi \times u$  for (a)  $P_R = 0.002$  and (b)  $P_R = 0.006$ . The colour bar shows the values of  $\tau$ .

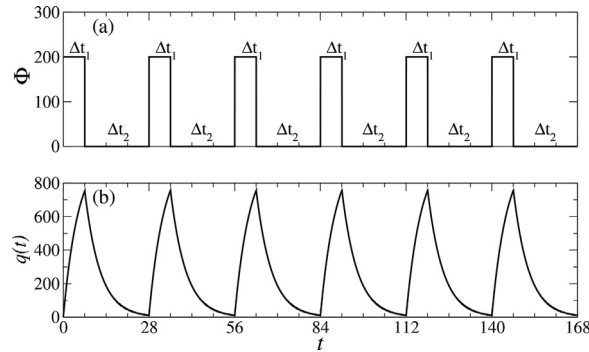


Fig. 6. (a) Intermittent schedule of the pulsed chemotherapy, where  $\Delta t_1$  and  $\Delta t_2$  are the time intervals with (days on) and without (days off) chemotherapy, respectively. (b) Temporal evolution of the drug concentration  $q(t)$ .

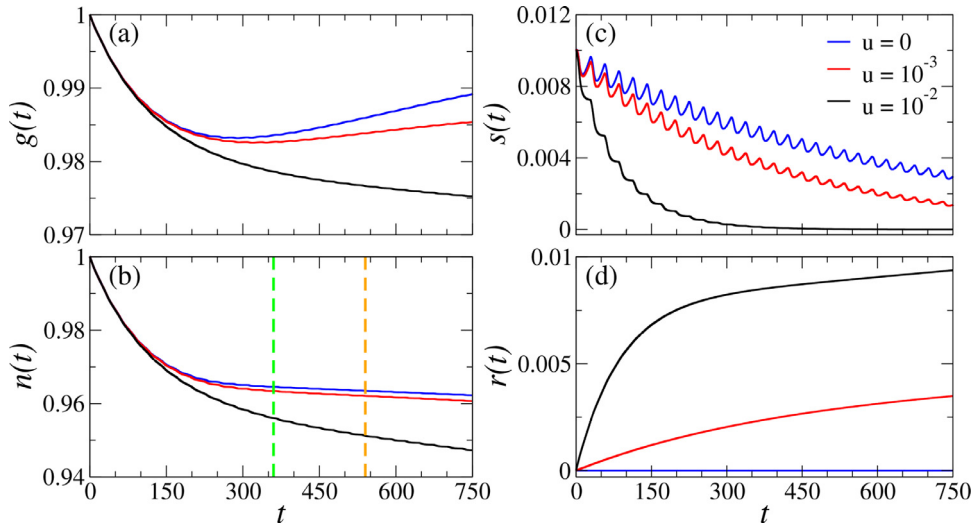
We also calculate  $\tau$  by varying  $\Phi$  and  $u$ , as shown in Fig. 5. The colour bar represents the values of  $\tau$ . In our simulations, the blue region corresponds to  $\tau$  greater than 700 days. In the orange, black, and red regions, the  $\tau$  values are for about 650, 500 and 350 days, respectively. The  $\tau$  values less than 300 days are in the green region. Fig. 5(a), for  $P_R = 0.002$ , is separated into four regions denoted by I, II, III, and IV. In the region I, we have  $s(t) < 0.01$  and  $r(t) < 0.01$ , namely, when  $n = 0.9$  both sensitive and resistant gliomas have a concentration less than the initial glioma concentration. Region II,  $s(t) < 0.01$  and  $r(t) > 0.01$ , shows that only the sensitive glioma is suppressed. The sensitive glioma grows in region III,  $s(t) > 0.01$  and  $r(t) < 0.01$ . In the region IV, both sensitive and resistant glioma have a concentration greater than the initial glioma concentration,  $s(t) > 0.01$  and  $r(t) > 0.01$ . For  $P_R = 0.006$  and  $\Phi \leq 200$  (Fig. 5(b)), there is no region I.

### 3.2. Pulsed chemotherapy

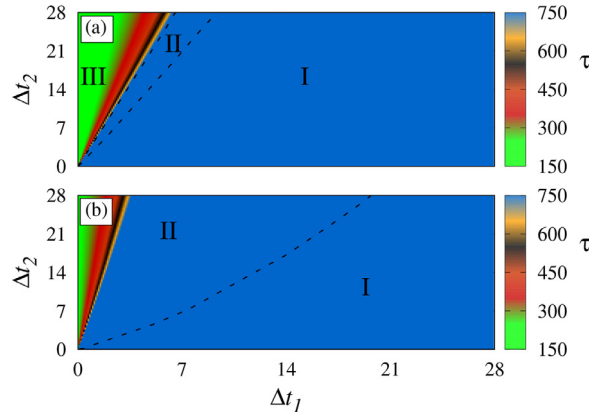
Pulsed chemotherapy is the use of intermittent schedules of chemotherapeutic agents to treat cancer [42]. Researchers have been carrying out various treatment types with different protocols to eliminate cancerous cells. In the literature, one finds results based on theoretical studies [43,44] and experiments [45–47]. Our intermittent schedule is illustrated in Fig. 6(a), where  $\Delta t_1$  and  $\Delta t_2$  correspond to the time intervals with (days on) and without (days off) chemotherapy, respectively. Fig. 6(b) displays the temporal evolution of  $q(t)$ . We observe an exponential growth of drug concentration  $q(t)$  during the drug application and an exponential decay after the application.

Fig. 7 shows (a)  $g(t)$ , (b)  $n(t)$ , (c)  $s(t)$ , and (d)  $r(t)$  for  $\Delta t_1 = 7$  days with  $\Phi = 200$  and  $\Delta t_2 = 21$  days. We consider  $P_R = 0.002$ ,  $u = 0$  (blue line),  $u = 10^{-3}$  (red line), and  $u = 10^{-2}$  (black line). At  $t = 360$  days (green vertical dashed line), we find  $n = 0.964$ ,  $n = 0.963$ , and  $n = 0.956$  for  $u = 0$ ,  $u = 10^{-3}$ , and  $u = 10^{-2}$ , respectively. When  $t = 540$  days,  $n = 0.963$  for  $u = 0$ ,  $n = 0.962$  for  $u = 10^{-2}$ , and  $n = 0.951$  for  $u = 10^{-2}$ . In this intermittent schedule, the  $n$  values are less than by considering the continuous chemotherapy.

There are many types of treatment schedules. With this in mind, we vary the number of days on and days off to analyse the effects of the drug resistance on different chemotherapy protocols. Fig. 8 exhibits  $\tau$  (colour bar) as a function of  $\Delta t_2 \times \Delta t_1$ . In Fig. 8(a), we verify the existence of the four regions, where the region IV is very small and it is between the regions II and III. For  $u = 10^{-2}$ , there are only the regions I and II, as shown in Fig. 8(b). The region I is larger for  $u = 10^{-3}$  (Fig. 8(a)) than for  $u = 10^{-2}$  (Fig. 8(b)). Therefore, the region I decreases and the region II increases when  $u$  increases, i.e., the number of treatment schedules that control the growth of both sensitive and resistant glioma cells decreases.



**Fig. 7.** Time evolution of (a)  $g(t)$ , (b)  $n(t)$ , (c)  $s(t)$ , and (d)  $r(t)$  for  $\Delta t_1 = 7$  days with  $\Phi = 200$  and  $\Delta t_2 = 21$  days with  $\Phi = 0$ ,  $P_R = 0.002$ ,  $u = 0$  (blue line),  $u = 10^{-3}$  (red line), and  $u = 10^{-2}$  (black line). The green and orange vertical dashed lines correspond to 360 and 540 days, respectively. (For interpretation of the references to color in this figure legend, the reader is referred to the web version of this article.)



**Fig. 8.**  $\Delta t_2 \times \Delta t_1$  for  $P_R = 0.002$ , (a)  $u = 10^{-3}$ , and (b)  $u = 10^{-2}$ . The colour bar shows the values of  $\tau$ .

#### 4. Conclusions

There are many different types of brain tumours. The treatments depend on the tumour characteristics. One of the most common malignant tumours in the brain is the glioma. This tumour begins in the glial cells and affects the support of the neurons. Due to this fact, without support and protection, the number of neurons decreases.

We extend the mathematical model of brain tumour growth proposed by Iarosz et al. [30]. This model describes glianeuron interaction and chemotherapy treatment. In this work, we modify the model by splitting the equation of the glioma cells into two equations. The new equations correspond to sensitive and resistant glioma cells.

We consider continuous and pulsed chemotherapy to destroy glioma cells without harming a large number of neurons. With regard to the continuous chemotherapy, the time  $\tau$  to achieve  $n = 0.9$  decreases when the mutation rate  $u$  from sensitive to resistant glioma cells increases. The  $\tau$  values depend on  $\Phi$  and  $u$ . For small  $P_R$  values, we find values in the parameter space  $\Phi \times u$  (region I), where the continuous chemotherapy kills both sensitive and resistant gliomas. In the pulsed chemotherapy, the region for the best treatment, according to days on and days off, decreases for larger  $u$  values.

#### Declaration of Competing Interest

None.

#### CRediT authorship contribution statement

**José Trobia:** Formal analysis, Investigation. **Kun Tian:** Investigation. **Antonio M Batista:** Supervision, Writing – original draft, Writing – review & editing. **Celso Grebogi:** Writing – review & editing. **Hai-Peng Ren:** Writing – review & editing.



ing. **Moises S Santos:** Methodology. **Paulo R Protachevicz:** Investigation, Methodology. **Fernando S Borges:** Investigation, Methodology. **José D Szezech Jr.:** Writing – review & editing. **Ricardo L Viana:** Writing – review & editing. **Iberê L Caldas:** Writing – review & editing. **Kelly C Iarosz:** Formal analysis, Investigation, Methodology.

## Acknowledgments

We wish to acknowledge the support: Araucária Foundation, National Council for Scientific and Technological Development (CNPq, 302665/2017-0 and 407299/2018-1), Coordination for the Improvement of Higher Education Personnel (CAPES), and São Paulo Research Foundation (Processes 2015/07311-7, 2017/18977-1, 2018/03211-6, 2020/04624-2). The authors would like to thank the 105 Group Science ([www.105groupscience.com](http://www.105groupscience.com)) for the fruitful discussions.

## References

- [1] Cooper GM. The development and causes of cancer. The cell: a molecular approach 2nd edition Sunderland (MA), Sinauer Associates; 2000.
- [2] Perry MC. The chemotherapy source book. Baltimore: Williams & Wilkins; 2008.
- [3] Tubiana M. Tumor cell proliferation kinetics and tumor growth rate. *Acta Oncol* 1989;28:113–21.
- [4] Karlsson P, Cole BF, Price KN, Gelber RD, Coates AS, Goldhirsch A, Castiglione M, Colleoni M, Gruber G. Timing of radiation therapy and chemotherapy after breast-conserving surgery for node-positive breast cancer: long-term results from international breast cancer study group trial VI and VII. *Int J Radiat Oncol Biol Phys* 2016;96:273–9.
- [5] López AG, Iarosz KC, Batista AM, Seoane JM, Viana RL, MAF S. The dose-dense principle in chemotherapy. *J Theor Biol* 2017;430:169–76.
- [6] López AG, Iarosz KC, Batista AM, Seoane JM, Viana RL, MAF S. Nonlinear cancer chemotherapy: modelling the Norton-Simon hypothesis. *Commun Nonlinear Sci Numer Simul* 2019;70:307–17.
- [7] López AG, Iarosz KC, Batista AM, Seoane JM, Viana RL, MAF S. The role of dose density in combination cancer chemotherapy. *Commun Nonlinear Sci Numer Simul* 2019;79:104918.
- [8] Pinho STR, Freedman HI, Nani F. A chemotherapy model for the treatment of cancer with metastasis. *Math Comput Model* 2002;36:773–803.
- [9] Borges FS, Iarosz KC, Ren HP, Batista AM, Baptista MS, Viana RL, Lopes SR, Grebogi C. Model for tumour growth with treatment by continuous and pulsed chemotherapy. *BioSystems* 2014;116:43–8.
- [10] Nani F, Freedman HI. A mathematical model of cancer treatment by immunotherapy. *Math Biosci* 2000;163:159–99.
- [11] de Pillis LG, Radunskaya AE, Wiseman CL. A validated mathematical model of cell-mediated immune response to tumor growth. *Cancer Res* 2005;65:7950–8.
- [12] Behera A, O'Rourke SFC. The effect of correlated noise in a Gompertz tumor growth model. *Braz J Phys* 2008;38:272–8.
- [13] Wang Z, Xu Y, Li Y, Kapitaniak T, Kurths J. Chimera states in coupled Hindmarsh-Rose neurons with  $\alpha$ -stable noise. *Chaos Soliton Fract* 2021;148:110976.
- [14] Zhang XY, Xu Y, Liu Q, Kurths J. Rate-dependent tipping-delay phenomenon in a thermoacoustic system with colored noise. *Sci China Technol Sci* 2020;63. doi:10.1007/s11431-020-1589-x.
- [15] Ma J, Xu Y, Li Y, Tian R, Ma S, Kurths J. Quantifying the parameter dependent basin of the unsafe regime of asymmetric Lévy-noise-induced critical transitions. *Appl Math Mech* 2021;42:65–84.
- [16] Wang Z, Xu Y, Li Y, Kurths J.  $\alpha$ -stable noise-induced coherence on a spatially extended Fitzhugh-Nagumo system. *J Stat Mech* 2019;2019:103501.
- [17] Wang Z, Xu Y, Li Y, Kurth J. The probability density function of interspike intervals in an FHN model with  $\alpha$ -stable noise. *Eur Phys J Plus* 2021;136:299.
- [18] Ma J, Xu Y, Liu D, Tian R, Ma S, Feudel U, Kurths J. Suppression of noise-induced critical transitions: a linear augmentation method. *Eur Phys J Spec Top* 2021. doi:10.1140/epjs/s11734-021-00112-1.
- [19] Tian R, Zhao Z, Xu Y. Variable scale-convex-peak method for weak signal detection. *Sci China Technol Sci* 2021;64:331–40.
- [20] Stupp R, Hegi ME, Gilbert MR, Chakravarti A. Chemoradiotherapy in malignant glioma: standard of care and future directions. *J Clin Oncol* 2007;25:4127–36.
- [21] Jäkel S, Dimou L. Glial cells and their function in the adult brain: a journey through the history of their ablation. *Front Cell Neurosci* 2017;11:1–17.
- [22] Peters GJ. Cancer drug resistance: a new perspective. *Cancer Drug Resist* 2018;1:1–5.
- [23] Housman G, Byler S, Heerboth S, Lapinska K, Longacre M, Snyder N, Sarkar S. Drug resistance in cancer: an overview. *Cancers* 2014;6:1769–92.
- [24] Nass J, Efferrth T. Drug targets and resistance mechanisms in multiple myeloma. *Cancer Drug Resist* 2018;1:87–117.
- [25] He YJ, Meghani K, M-C C, Yang C, Ronato DA, Bian J, Sharma A, Moore J, Niraj J, Detappe A, Doench JG, Legube G, Root DE, D'Andrea AD, Drané P, S D, Konstantinopoulos PA, J-Y M, Chowdhury D. DYNLL1 binds to MRE11 to limit DNA end resection in BRCA1-deficient cells. *Nature* 2018;563:522–6.
- [26] Rockne R, Alvord JEC, Rockhill JK, Swanson KR. A mathematical model for brain tumor response to radiation therapy. *J Math Biol* 2009;58:561–78.
- [27] Kansal AR, Torquato S, Chiozza EA, Deisboeck TS. Emergence of a subpopulation in a computational model of tumor growth. *J Theor Biol* 2000;207:431–41.
- [28] Sun X, Bao J, Shao Y. Mathematical modeling of therapy-induced cancer drug resistance: connecting cancer mechanisms to population survival rates. *Sci Rep* 2016;6:22498.
- [29] Haroun RI, Clatterbuck RE, Gibbons MC, Burger PC, Parker R, Fruehauf JP, Brem H. Extreme drug resistance in primary brain tumors: in vitro analysis of 64 resection specimens. *J Neurooncol* 2002;58:115–23.
- [30] Iarosz KC, Borges FS, Batista AM, Baptista MS, RAN S, Viana RL, Lopes SR. Mathematical model of brain tumour with glia-neuron interactions and chemotherapy treatment. *J Theor Biol* 2015;368:113–21.
- [31] Rabé M, Dumont S, Álvarez-Arenas A, Janati H, Belmonte-Beitia J, Calvo GF, Thibault-Carpentier C, Séry Q, Chauvin C, Joalland N, Briand F, Blandi S, Scotet E, Pecqueur C, Clairambault J, Oliver L, Perez-Garcia V, Nadaradjane A, P-F C, Gratas C, Vallette FM. Identification of a transient state during the acquisition of temozolomide resistance in glioblastoma. *Cell Death Dis* 2020;11:19.
- [32] STR P, Barcelar FS, RFS A, Freedman HI. A mathematical model for the effect of anti-angiogenic therapy in the treatment of cancer tumours by chemotherapy. *Nonlinear Anal Real World Appl* 2013;14:815–28.
- [33] Spratt JS, Spratt TL. Rates of growth of pulmonary metastases and host survival. *Ann Surg* 1964;159:161–71.
- [34] Rzeski W, Pruski S, Macke A, Felderhoff-Mueser U, Reiher AK, Hoerster F, Jansma C, Jarosz B, Stefovská V, Bittigau P, Ikonomidou C. Anticancer agents are potent neurotoxins in vitro and in vivo. *Ann Neurol* 2004;56:351–60.
- [35] Stupp R, Mason WP, Van den Bent MJ, Weller M, Fisher B, MJB T, Belanger K, Brandes AA, Marosi C, Bogdahn U, Curschmann J, Janzer RC, Ludwin SK, Gorlia T, Allgeier A, Lacombe D, Cairncross JG, Eisenhauer E, Mirimanoff RO. Radiotherapy plus concomitant and adjuvant temozolomide for glioblastoma. *N Engl J Med* 2005;352:987–96.
- [36] Strik HM, Marosi C, Kaina B, Neyns B. Temozolomide dosing regimens for glioma patients. *Curr Neurol Neurosci Rep* 2012;12:286–93.
- [37] FAC A, LRB C, Grinberg LT, Farfel JM, REL F, REP L, Filhos WJ, Lent R, Herculano-Houzel S. Equal numbers of neuronal and nonneuronal cells make the human brain an isometrically scaled-up primate brain. *J Comp Neurol* 2009;513:532–41.
- [38] Vogelzang NJ. Continuous infusion chemotherapy: a critical review. *J Clin Oncol* 1984;2:1289–304.
- [39] Rotman M, Rosenthal CJ. Concomitant continuous infusion chemotherapy and radiation. Berlin: Springer-Verlag; 1991.
- [40] Lai J, Xu P, Jiang X, Zhou S, Liu A. Successful treatment with anti-programmed-death-1 antibody in a relapsed natural killer/t-cell lymphoma patient with multi-line resistance: a case report. *BMC Cancer* 2017;17:507.

- [41] Peters A, Morrison JH, Rosene DL, Hyman BT. Are neurons lost from the primate cerebral cortex during normal aging. *Cereb Cortex* 1998;8:295–300.
- [42] Beer TM, Garzotto M, Hennen WD, Eilers KM, Wersinger EM. Multiple cycles of intermittent chemotherapy in metastatic androgen-independent prostate cancer. *Br J Cancer* 2004;91:1425–7.
- [43] Foo J, Michor F. Evolution of resistance to targeted anti-cancer therapies during continuous and pulsed administration strategies. *PLoS Comput Biol* 2009;5:e1000557.
- [44] H-P R, Yang Y, Baptista MS, Grebogi C. Tumour chemotherapy strategy based on impulse control theory. *Philos Trans R Soc A* 2017;375:20160221.
- [45] Wasan H, Meade AM, Adams R, Wilson R, Pugh C, Fisher D, Sydes B, Madi A, Sizer B, Lowdell C, Middleton G, Butler R, Kaplan R, Maughan T. Intermittent chemotherapy plus either intermittent or continuous cetuximab for first-line treatment of patients with KRAS wild-type advanced colorectal cancer (COIN-b): a randomised phase 2 trial. *Lancet Oncol* 2014;14:631–9.
- [46] AKM C, FLG E, Lopez-Yurda M, Bouma JM, Rademaker Lakhai JM, Honkoop AH, de Graaf H, VCG T-H, MEMM B. on behalf of the dutch breast cancer research group (BOOG). secondary analyses of the randomized phase III Stop&Go study: efficacy of second-line intermittent versus continuous chemotherapy in HER2-negative advanced breast cancer. *Acta Oncologica* 2020;59:713–22.
- [47] Du B, Waxman DJ. Medium dose intermittent cyclophosphamide induces immunogenic cell death and cancer cell autonomous type I interferon production in glioma models. *Cancer Lett* 2020;470:170–80.